Available online at www.sciencedirect.com
ScienceDirect
Tetrahedron 63 (2007) 10290–10299
Tetrahedron

New 3-hydroxyflavone derivatives for probing hydrophobic sites in microheterogeneous systems

Turan Ozturk,[a,*] Andrey S. Klymchenko,[b] Asli Capan,[a] Sule Oncul,[c] Simay Cikrikci,[a] Sule Taskiran,[a] Bahar Tasan,[a] F. Betul Kaynak,[d] Suheyla Ozbey[d] and Alexander P. Demchenko[c,e]

[a]*Department of Chemistry, Science Faculty, Istanbul Technical University, Maslak, Istanbul, Turkey*
[b]*Département de Pharmacologie et Physicochimie, Photophysique des Interactions Biomolécularies, UMR7175, Institut Gilbert Laustriat, Université Louis Pasteur (Strasbourg I), BP 60024, 76401 Illkirch, France*
[c]*TUBITAK Research Institute for Genetic Engineering & Biotechnology, Gebze-Kocaeli, Turkey*
[d]*Department of Engineering Physics, Hacettepe University, Beytepe, Ankara, Turkey*
[e]*Palladin Institute of Biochemistry, Kiev, Ukraine*

Received 16 March 2007; revised 9 July 2007; accepted 20 July 2007
Available online 29 July 2007

Abstract—Nine new 3-hydroxyflavone derivatives as fluorescent molecular sensors having two well-separated emission bands were synthesized. These sensors can occupy well-determined locations and orientations in macromolecular ensembles, such as micelles due to their finely-tuned designs. These polarity-sensitive dyes can incorporate into the anhydrous hydrophobic core of aqueous micelles.

1. Introduction

3-Hydroxyflavones (3HF) **1** are important candidates as fluorescent molecular sensors since they have interesting fluorescent properties, resulting from their excited state intramolecular proton transfer (ESIPT) reaction.[1] This property leads to two well-separated, highly intense and solvent-dependent emission bands, the ratio of the intensities of which is strongly sensitive to the polarity and hydrogen bonding perturbations[1c] in proteins,[2] micelles[3] and polymers.[4] These bands originate from the normal excited form (N*) and the phototautomer (T*).[1a,5] It has been disclosed that the introduction of an electron donor group to the 4′-position of the 3HF increases the sensitivity of fluorescence spectra of the molecule, which has attracted the interest of research groups as two-band fluorescent dyes with a ratiometric response to different perturbations.[6] This resulted in a variety of applications for substituted 3HFs as ion sensors[7] and probes in the studies of organized systems such as micelles[8] and phospholipid vesicles.[3,9]

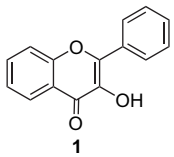

1

Our recent investigations[10] to understand the behaviour of 3HFs with regard to their interaction with living cells, indicated that 3HFs can enter into lipid bilayers.[11] Their application has dramatically increased in recent years—from studies on effects of solubilization of water in reverse micelles[8b] and inclusion complexes with cyclodextrins[12] to the studies of supercritical liquids.[13] These results have stimulated new efforts to synthesize improved compounds with the ability to occupy well-determined locations and orientations in macromolecular ensembles, such as micells and phospholipid bilayers. This led us to design a series of finely-tuned compounds **21**–**29** with prospective application in the studies of living cells. Development of such probes is very important since the fast detection of bio-pollution in the environment is desirable. Additionally, an X-ray structure of 3HF is disclosed in this work, which gives insight into the planarity of the molecule.

2. Results and discussion

2.1. Synthesis

The synthesis of finely-tuned 3HFs was carried out through the modified Algar–Flyn–Oyamada (AFO) reaction.[6g,14] The aldehydes **6**–**8** were synthesized from aniline **2**, which was dialkylated with iodobutane, iodohexane and iodooctane to obtain the dialkylanilines **3**–**5**, respectively, and subsequent formylation with phosphoryl trichloride–DMF resulted in the production of the aldehydes (Scheme 1).

* Corresponding author. E-mail: ozturktur@itu.edu.tr

0040–4020/$ - see front matter © 2007 Published by Elsevier Ltd.
doi:10.1016/j.tet.2007.07.074

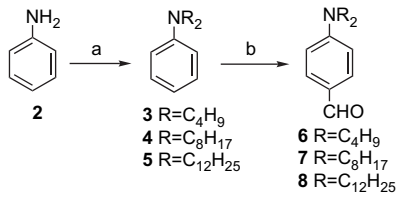

Scheme 1. (a) R–I, K_2CO_3, acetone, reflux and (b) $POCl_3$–DMF, 0→60 °C.

While the acetophenones **9** and **10** are commercially available, the ketone, 4-octyloxyacetophenone **11** was prepared following the reaction conditions applied for the synthesis of the alkylanilines **3**–**5**. Condensation of the aldehydes **6**–**8** with the acetophenones **9**–**11**, using sodium methoxide as base in place of sodium hydroxide, which is the main modification of AFO reaction, gave intermediates **12**–**20** in 5 h, rather than nearly one week in the AFO reaction (Scheme 2). The ring closure reaction was performed on the intermediate without any isolation. To the reaction mixture was added excess sodium methoxide and hydrogen peroxide at 0 °C, then it was heated to boiling and kept at that temperature for around 5 min. Isolation was achieved using column chromatography, which gave the fluorescent 3HFs **21**–**29**.

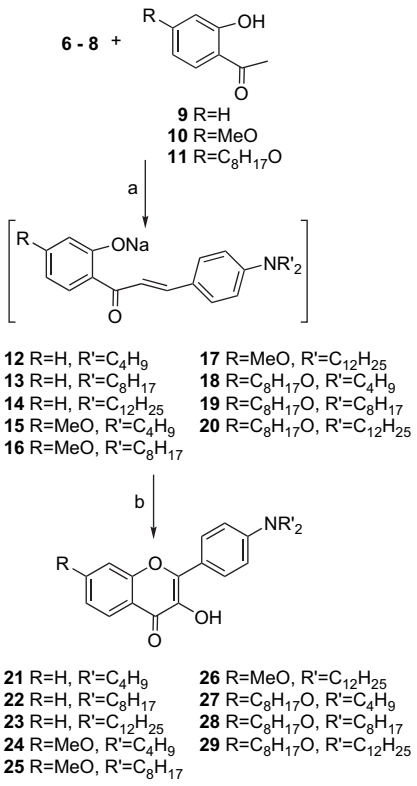

Scheme 2. (a) MeONa, EtOH, rt and (b) H_2O_2/MeONa, 0 °C→reflux.

2.2. Solvent-dependent variations of spectra

The influence of solvent on the absorption and fluorescence spectra is illustrated for one of the synthesized dyes, **28** (Fig. 1). A smooth absorption band located in the region of 400 nm exhibiting significant solvent-dependent shifts, and in fluorescence spectra, two bands, typical feature of 3-hydroxychromones were observed. The N* band located at

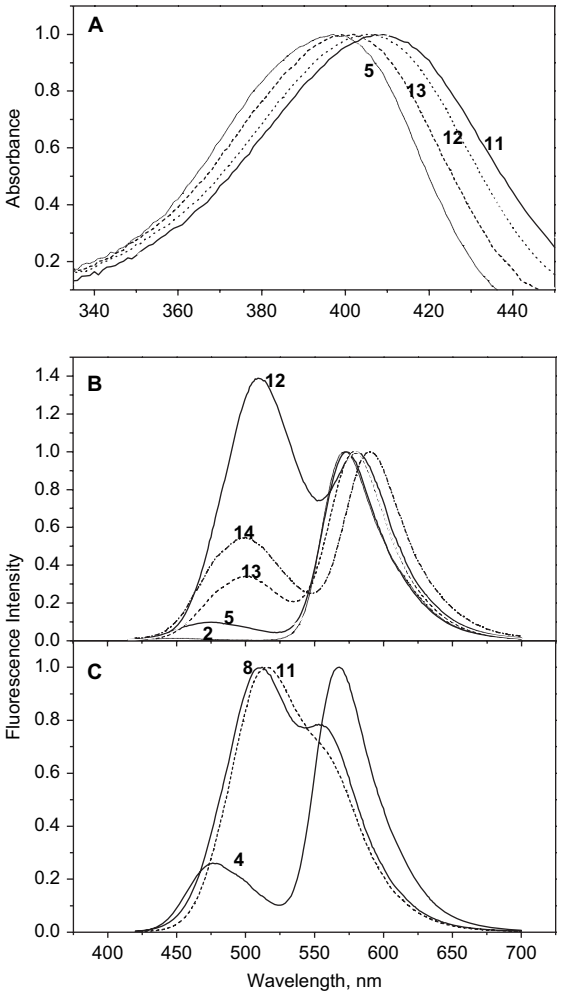

Figure 1. Normalized absorption (A) and fluorescence emission spectra of **28** (B and C) in aprotic solvents (B) and in protic solvents (C). Solvents are numbered according to Table 1.

shorter wavelengths exhibits dramatic change of its intensity relative to the T* band located at longer wavelengths. A spectral shift to longer wavelength accompanies an increase of relative intensity of N* band. This shift is especially strong in protic solvents such as butanol and ethanol so that the T* band becomes poorly resolved and is observed as shoulders. According to the commonly accepted model of 3HF photophysics, the N* band belongs to the initially excited species and the T* band to the product of ESIPT reaction. Strong solvent-dependent sensitivity of the spectrum indicates the strong influence of solute–solvent interactions in the ground and excited states. Since it is known that the spectra of 3HFs are very sensitive to the hydrogen bonding of proton–donor groups of solvents with 4-carbonyl functionality, and that their dipole moments increase dramatically on excitation favouring the strong effects of solvent polarity, significant differences between fluorescence spectra in aprotic and protic solvents and also in solvents of different polarities were expected and experimentally observed (Fig. 1).

Solvent-dependent spectroscopic behaviours of three representatives **22**, **25** and **28**, having equal lengths of hydrocarbon chains, of three synthesized 3HF families were studied

in detail (Table 1). A strong correlation of the position of absorption band maxima on electronic polarizability function $f(n)$ (where n is the refraction index) and of the position of N* band on polarity function $f(\varepsilon)$ (where ε is the dielectric constant) was observed. These results were illustrated by plotting corresponding graphs.

In Figure 2, the results were compared using the plots of position of fluorescence band maximum on energy scale (in cm^{-1}) versus the function $f(n)$. It was observed that all the points corresponding to the solvents with proton–donor and proton–acceptor properties lie below the lines drawn for neutral solvents. This indicates that specific solute–solvent interactions always shift the absorption spectra to longer wavelengths. And, in general, this effect is stronger than the effect of electronic polarizability, which is found to be common behaviour among the studied compounds. On the other hand, positions of the fluorescence spectra depend more strongly on solvent polarity (Fig. 3). For both N* and T* bands, the spectra shift to longer wavelengths with the increase of $f(\varepsilon)$, but for N* band this dependence is much stronger compare to the T* band. Such behaviour of the three compounds, **22**, **25** and **28**, was noticed to be similar. The band positions do not show a strong dependence on the formation of intermolecular hydrogen bond by the carbonyl groups of the studied probes that occur in protic solvents. This observation is in line with the previous results[6h] obtained for a similar 3HF derivative having a simpler structure (4′-diethylamino-3-hydroxyflavone) for which the detailed spectroscopic data obtained in 21 solvents were analyzed. Therefore, the major effect on the positions of the spectral bands is the solvent polarity.

Table 1. Spectroscopic properties of the studied 3-hydroxyflavone derivatives in different solvents[a]

	Solvent	3HF	$f(\varepsilon)$	$f(n)$	α	β	λ_{abs} (nm)	λ_{N^*} (nm)	λ_{N^*} (nm)	I_{N^*}/I_{T^*}
1	Hexane	**22**	0.1849	0.1862	0.00	0.00	406	428	556	0.01
		25					397	415	563	0.01
		28					397	431	566	0.01
2	Toluene	**22**	0.2387	0.2261	0.00	0.14	410	458	567	0.04
		25					402	449	572	0.01
		28					402	457	572	0.01
3	Anisole	**22**	0.3413	0.2324	0.00	0.29	412	477	574	0.02
		25					406	460	578	0.07
		28					403	468	578	0.04
4	Chloroform	**22**	0.3563	0.2104	0.15	0.02	417	485	565	0.68
		25					409	474	568	0.26
		28					409	476	568	0.26
5	Ethyl acetate	**22**	0.3850	0.1853	0.00	0.45	406	483	571	0.36
		25					396	462	575	0.62
		28					397	475	573	0.1
6	Tetrahydrofuran	**22**	0.4074	0.1977	0.00	0.48	406	477	577	0.22
		25					399	456	579	0.07
		28					396	457	579	0.05
7	Dichloromethane	**22**	0.4217	0.2032	0.10	0.05	415	496	571	0.68
		25					406	480	576	0.2
		28					407	479	575	0.15
8	*n*-Butanol	**22**	0.4574	1.1955	0.37	0.48	415	515	—	—
		25					405	511	551	1.39
		28					411	511	553	1.27
9	Isopropanol	**22**	0.4601	0.1862	0.33	0.56	413	511	—	—
		25					409	506	555	1.38
		28					407	505	558	1.21
10	Acetone	**22**	0.4647	0.1804	0.04	0.49	407	505	576	0.99
		25					399	482	580	0.19
		28					400	482	580	0.17
11	Ethanol	**22**	0.4704	0.1812	0.37	0.48	413	526	—	—
		25					405	514	—	—
		28					409	516	—	—
12	*N*,*N*-Dimethylformamide	**22**	0.4798	0.2043	0.00	0.74	410	510	583	1.43
		25					401	528	583	0.87
		28					405	509	580	1.39
13	Acetonitrile	**22**	0.4802	0.1747	0.07	0.32	407	510	572	1.33
		25					400	501	579	0.36
		28					402	501	579	0.34
14	Dimethyl sulfoxide	**22**	0.4842	0.2199	0.00	0.88	410	514	585	0.18
		25					409	500	590	0.67
		28					404	500	589	0.55

[a] α and β: Abraham's hydrogen bond acidity and basicity, respectively;[1,2] λ_{abs} is the position of absorption maximum, λ_{N^*} and λ_{T^*} are the positions of the fluorescence maxima of the N* and T* states. The data in brackets refer to poorly resolved maximum (shoulder).

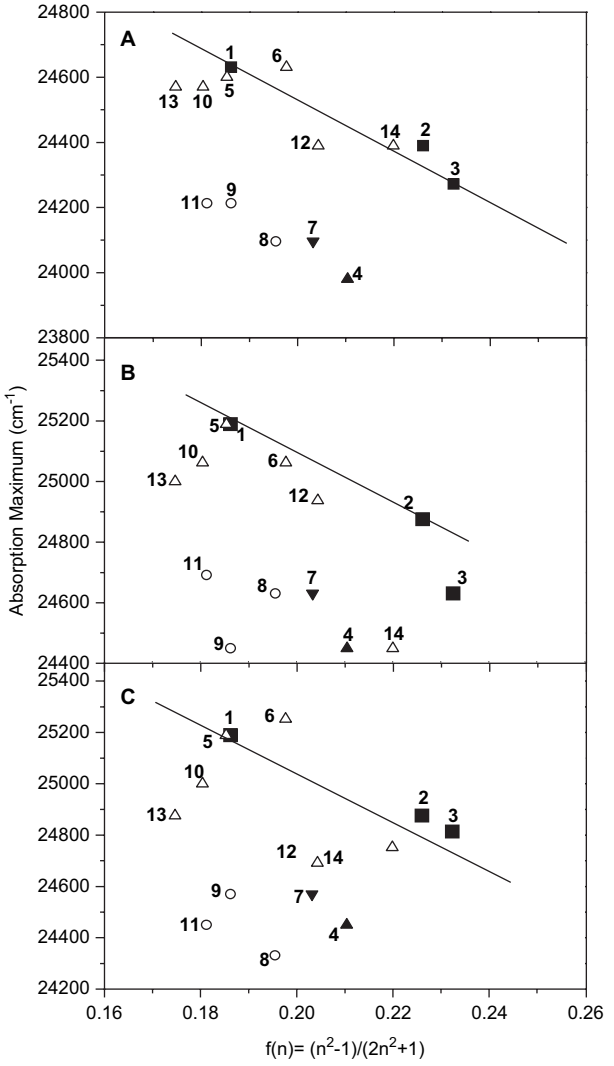

Figure 2. Position of absorption band maxima of studied flavones as a function of solvent polarizability, $f(n)$ in neutral (■), protic (○) and H-bond acceptor (△) solvents and also in chloroform (▲) and dichloromethane (▼). The probes are A: **22**, B: **25**, C: **28**. Solvents are numbered according to Table 1.

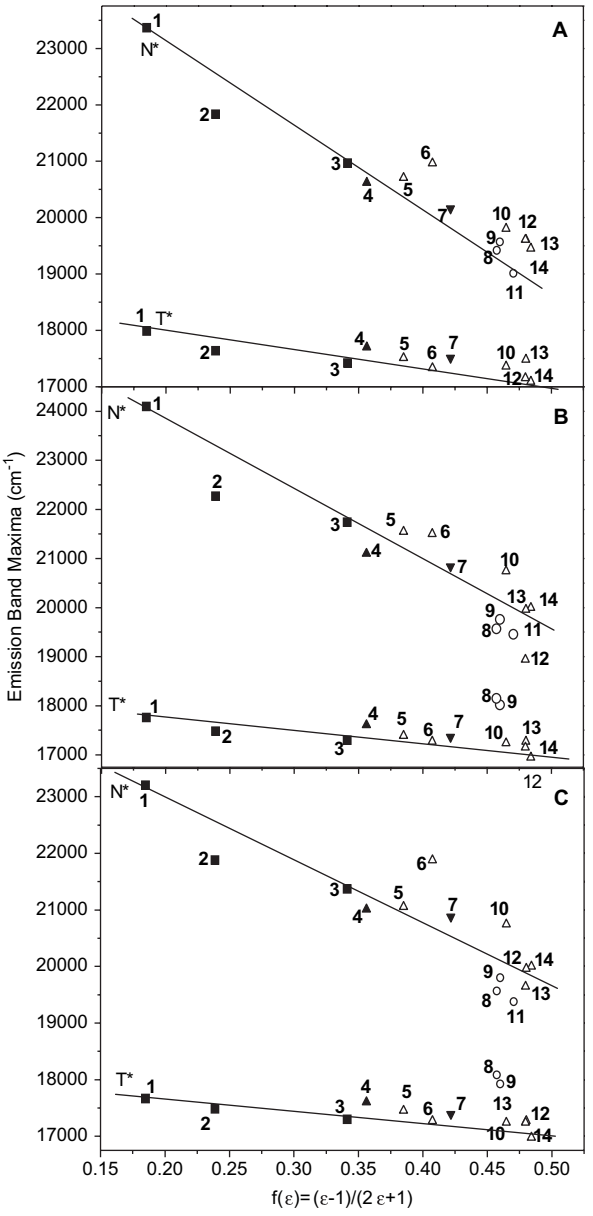

Figure 3. Position of N* and T* band maxima in fluorescence spectra as a function of polarity $f(\varepsilon)$ of different solvents. Symbols of the points correspond to that in Figure 2. The probes are A: **22**, B: **25**, C: **28**. Solvents are numbered according to Table 1.

As was found earlier for other functional 3HFs,[6a–g] the most significant solvent-dependent changes are observed for the relative intensities of the N* and T* bands (Fig. 4). The magnitude of these changes is so big that a logarithmic scale for displaying the intensity ratios, $\log(I_{N^*}/I_{T^*})$, was applied. It was observed that the ratio increases with increasing solvent polarity $f(\varepsilon)$.

As was indicated earlier,[6h] intermolecular hydrogen bonding effects may produce an additional increase of band intensity ratio on the background of polarity effects. In the results of the present study in which the deconvolution of the spectra into individual components was not used, such dependence was not clearly seen. Analysis of specific solvent effect based on Abraham's solvent acidity 'α' and basicity 'β' parameters indicated that the positions of the N* and T* bands, particularly their intensity ratio, are strongly sensitive to hydrogen bonding. Increase of the solvent polarity and the formation of hydrogen bonds produce spectral changes in the same direction: the shift of N* band to a longer wavelength and the increase of N*/T* intensity ratio. This property can be applied to detect penetration of polar and protic solvents such as water into microscopic particles and nanocomposites.

2.3. Studies in micelles

Micelles formed by surfactant molecules are self-assembled structures that are characterized by a strong gradient of polarity from polar interface exposed to aqueous solvent to hydrophobic core formed by hydrocarbon chains. In addition to many industrial applications, such as micellar catalysis and biocatalysis, micelles serve as simple models of biomembranes and test systems for probe development for biomembrane research. Probes that incorporate into the hydrophobic core of micelles and biomembranes and report in a two-band

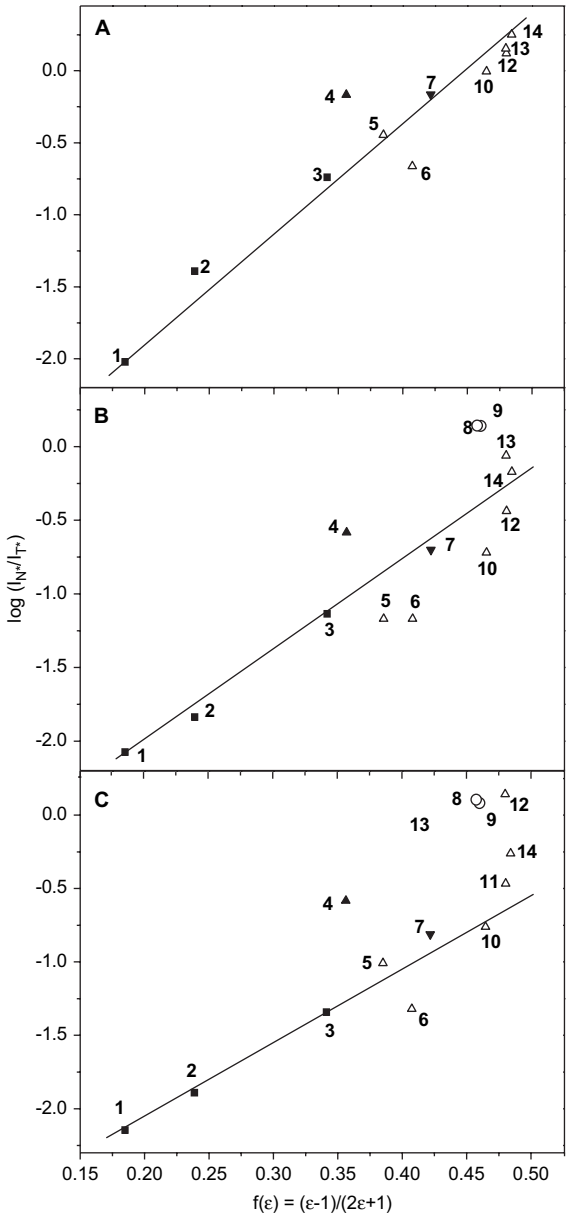

Figure 4. Logarithm of intensity ratio (I_{N^*}/I_{T^*}) versus polarity $f(\varepsilon)$ for different solvents. Symbols of the points correspond to that in Figure 2. The probes are A: **22**, B: **25**, C: **28**. Solvents are numbered according to Table 1.

wavelength-ratiometric manner on polarity and hydration at their binding sites are in high demand. For this reason we undertook a series of experiments on incorporation of synthesized dyes into micelles formed by cationic surfactant CTAB and neutral Triton X-100. Surprisingly, despite the similarity of structures of these dyes, divergent and therefore interesting results for their behaviour in these micelles were obtained.

In Triton X-100 micelles all the dyes incorporate well into micelles and show an increase of intensity from almost zero level observed in water (where most of them have a very low solubility) to a certain level, which reaches a maximum at concentrations corresponding to surfactant critical micelle concentrations (cmc). This level remains constant on further increase of surfactant concentration (data not shown). Probes **21**–**23** exhibit the highest fluorescence intensity with a variation of relative intensity of N* and T* fluorescence bands (Fig. 5, A–C). There is an important regularity: upon increase of chain length from **21** to **23**, the N* band compared to T* band (which is poorly resolved in **21**) changes dramatically; it decreases its relative intensity and moves to shorter wavelengths. This is a strong indication of changing the fluorophore environment—transition from more polar and hydrated sites to hydrophobic sites in micelle interior. The striking difference in response between the incorporated probes should be attributed to the effect of different substituents that verify the location of the fluorophore in the micelle structure. This interpretation is in line with the results obtained in model solvents that are presented above. It is logical to suggest that increase of the size of hydrophobic tail favours deeper location of fluorophore moiety into the micelle.

Quite contrasting results were obtained from the study on dyes of **24**–**26** and **27**–**29** series in the same, Triton X-100, micelles. For **24**, two bands of almost equal intensities were observed, and for **27** the T* band is substantially higher, which indicates a low polarity location of the dye. The tendency to decrease the relative intensity of the N* band on increasing the chain length is also observed for them. In addition, except **27**, these compounds exhibit substantially decreased relative intensity, which may be due to some quenching effect or some parts of the dye becoming aggregated in the micelle. However, this issue needs a more detailed investigation.

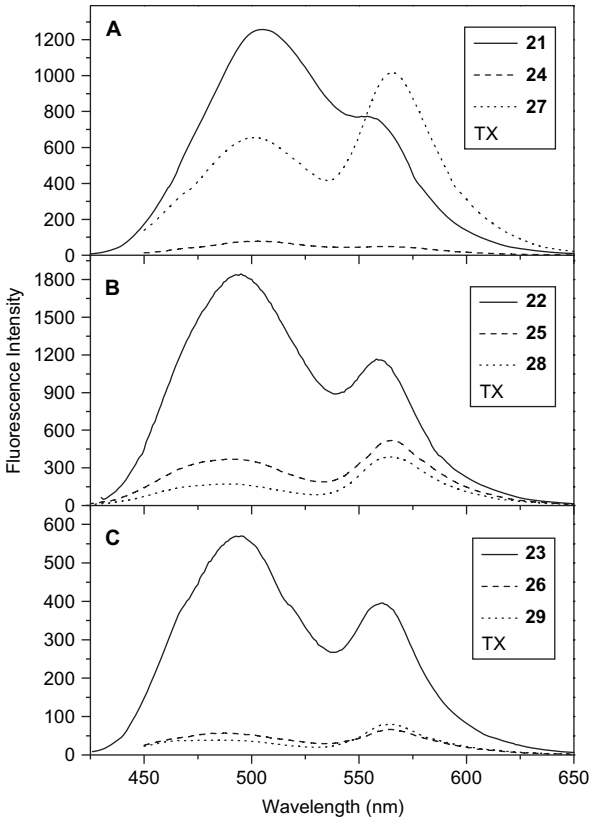

Figure 5. Fluorescence spectra of new dyes in Triton X-100 micelles formed in water.

Even more interesting results appear on the studies of new dyes in cationic detergent CTAB (Fig. 6, A–C). In the line of dyes **21**–**23** only a relatively intense N* band that is strongly shifted to longer wavelengths was observed. Thus, regardless of the length of the attached chain, the fluorophore is exposed to polar micelle surface and is highly hydrated (with 4-carbonyl group forming hydrogen bond with water). This conclusion is supported by our recently obtained data on the influence of hydrogen bonding with water on the fluorescence spectra of compounds of the same 3-hydroxyflavone family.[15]

Regarding the other studied compounds **24**–**29**, their relative fluorescence intensity is comparatively low (with the exception of **25**) or is dramatically quenched as for **26** and **29**. It is not excluded that these compounds incorporate into micelles in such a way that their fluorescence is quenched by collisions with bromide ions, which are known as a strong fluorescence quencher.[16] The dye **25** presents an exclusion due to its intense fluorescence spectrum with two bands being well resolved and of almost equal intensities, which indicates a moderately polar unhydrated fluorophore environment. The relatively narrow widths of these bands indicate the absence of heterogeneity of location of the studied probes (the distribution between the sites of different polarity and hydration), which in biomembrane studies was not achieved with 3HF probes having more simple structures.[17,18]

Thus, the synthesized dyes despite the same fluorophore incorporated into their structures display a variety of spectroscopic properties that are due to differences in their location and orientation in the micelles. Probes **27** and **25** are the most interesting for different micellar, bilayer structures and also apolar interfaces due to the possibility of hydrophobic location of their fluorophore unit. The low polarity of location of the probes is witnessed by the following facts. (i) Position of the most polarity-sensitive N* band corresponds to that in low-polar aprotic solvents (see Table 1). (ii) There is no evidence for the presence of the hydrogen-bonded forms of the dyes (that should have the spectrum strongly shifted to longer wavelengths). The micelle cores do not contain the groups that could be hydrogen bond donors, so the only expected partners for the formation of these bonds could be hydration water. Thus the probes are completely inaccessible to contact with water molecules. (iii) On the addition of iodide ions that are known as strong water-soluble collisional fluorescence quenchers, the quenching effect is not observed (data not shown). This fact is especially demonstrative for CTAB micelles since I^- ions can substitute Br^- ions in the polar interface layer thus increasing substantially their local concentration.

Thus, to our best knowledge this is the first example of successful incorporation of polarity-sensitive dye into the anhydrous hydrophobic core of an aqueous micelle. The previously applied more simple in structure 3HF derivatives did not achieve that goal. It is also known that many other applied probes of low polarity, such as aminonaphthalene, coumarin and aminophthalimide derivatives, are known to distribute in micelles between core and interface regions with a significant extent of hydrogen bonding to hydration water.[19–22]

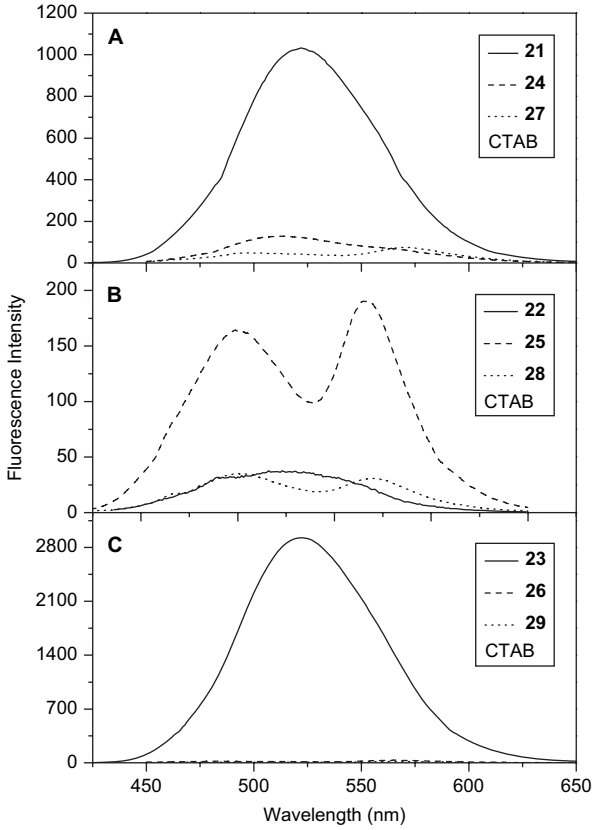

Figure 6. Fluorescence spectra of new dyes in CTAB micelles formed in water.

2.4. X-ray single crystal measurement

X-ray study reveals that in the crystal structure of **24** the asymmetric part of the unit cell contains two crystallographically independent molecules labelled A and B (Fig. 7). Both molecules are chemically equivalent but differ essentially in the conformation. As expected, the chromanone moiety of both molecules is planar i.e., the mean deviations of the atoms from the least-square squares planes are −0.048(5) and −0.055(5) Å for C4 and C3′ in A and B, respectively.

The phenyl ring and the chromanone moiety make a dihedral angle of 9.1(2)° in A, and the corresponding angle for B is

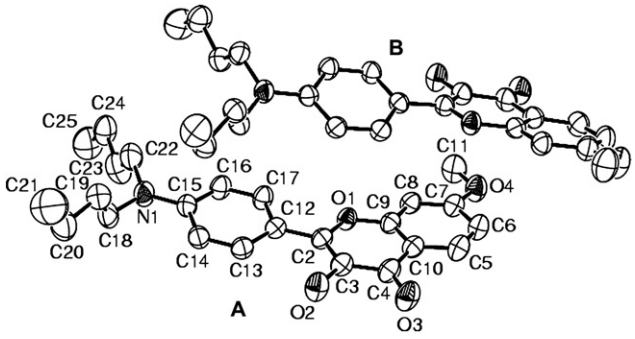

Figure 7. Perspective views of the asymmetric unit. Displacement ellipsoids are scaled to 30% probability level. Hydrogen atoms were not shown for clarity.

27.9(2)°, which reflects the major deviation from the planarity of the molecule. The value given for A is comparable with those of mikanin (7.9° in tetragonal form[23] and 9.2° in triclinic form[24] of the same molecule), flavone-3′-sulfonamide[25] (8.3°) and diethyl 2-6-dimethyl-4-(2-phenyl-4-oxo-4*H*-1-benzopyran-6-yl)-1,4-dihydropyridine-3,5-dicarboxylate[26] (10.7°), while the corresponding value for B is comparable with those of 3-hydroxy-3′-methylflavone[27] (23.1°) and 5-hydroxy-7-methoxyflavone[28] (24.8°). The coplanarity of the phenyl ring and the chromanone has been attributed to short intramolecular hydrogen contacts between H atoms of the phenyl and oxo groups of the pyran-4-one group. In flavones, generally, an increase of the dihedral angle means a decrease in the degree of conjugation between the C2–C12 bond and the π electrons of the pyran-4-one ring.

In molecule A, the methoxy group at C7 is nearly coplanar with the phenyl ring by the torsion angle C6–C7–O4–C11 176.7(4)°, whereas the methoxy group in B is slightly twisted out of the phenyl ring with the torsion angle of 167.7(4)°. The butyl groups at N1 are nearly orthogonal to the phenyl ring plane as indicated by the torsion angles C19–C18–N1–C15 82.8(5)° and C23–C22–N1–C15 101.0(5)° (90.4(4)° and 93.6(4)° in B).

The crystal structure of **24** is stabilized by intra- and intermolecular hydrogen bonds (Table 2). The packing of the molecules and the hydrogen bonding in the structure are shown in Figure 8. The two independent molecules exhibit the same pattern of hydrogen bonds except C17A–H17A···O1A intramolecular interaction in A, which contributes to the coplanarity of the phenyl ring with the rest of the molecule A. Chains of the molecules linked through O–H···O hydrogen bonds, which extend along the *b* axis, are joined by means of C11A–H11A···O2B bonds (Fig. 8).

3. Conclusion

With the aim of extending the possibilities of two-colour ratiometric environment-sensitive probes to localize selectively and to probe low-polar microenvironments we synthesized a number of 3-hydroxyflavone derivatives. They retain the major spectroscopic properties of parent compounds and, in addition, are able to incorporate selectively into low-polar environments. This is demonstrated in the studies of neutral and cationic micelles. However, the site and length of the hydrophobic substituent in the dye molecule, which has virtually no influence on spectroscopic properties in neat solvents can modulate significantly these properties in microheterogeneous systems such as micelles.

Table 2. Hydrogen-bonding geometry (Å, °) for **24**

D–H···A	D–H	H···A	D···A	D–H···A
O2A–H2A···O3A	0.82	2.27	2.704(4)	114
O2A–H2A···O3B$^{(i)}$	0.82	2.01	2.729(4)	146
O2B–H2B···O3B	0.82	2.30	2.736(4)	114
O2B–H2B···O3A$^{(i)}$	0.82	1.94	2.665(3)	148
C11A–H11A···O2B$^{(ii)}$	0.96	2.59	3.443(6)	148
C13A–H13A···O2A	0.93	2.17	2.826(4)	127
C13B–H13B···O2B	0.93	2.28	2.850(4)	119
C17A–H17A···O1A	0.93	2.36	2.702(4)	102

Symmetry codes: (i) $-x,-y,-z$ and (ii) $-x+1/2, y-1/2,-z+1/2$.

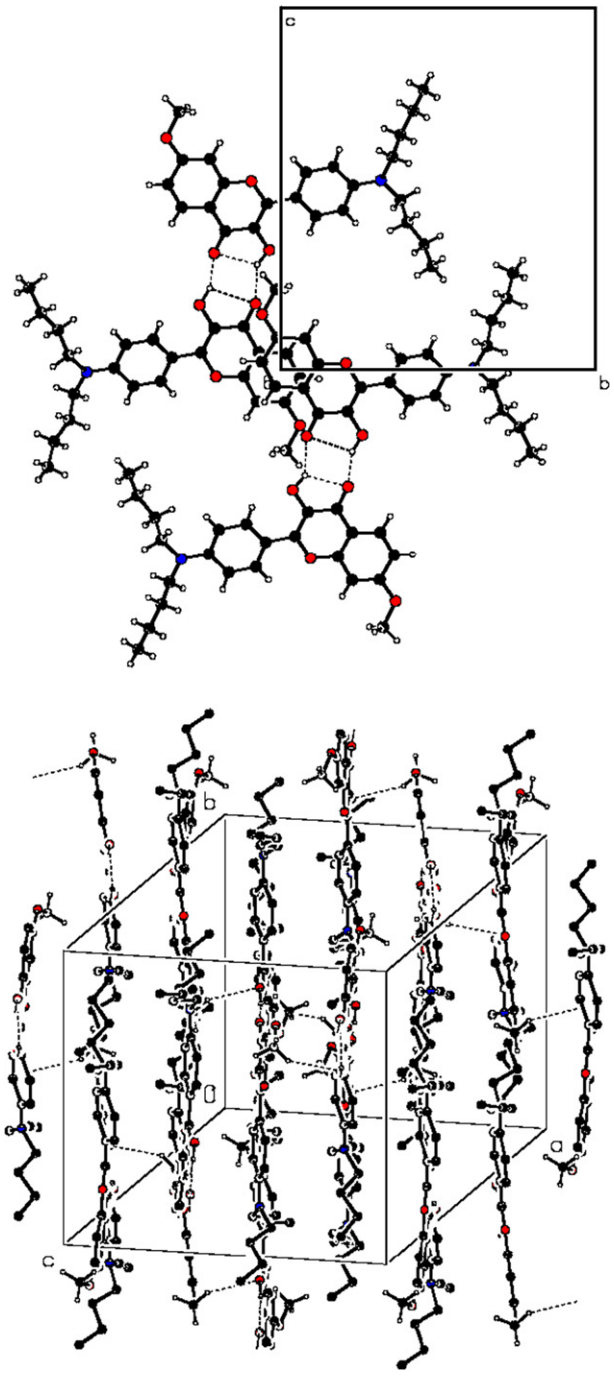

Figure 8. Compound **24** is viewed down the *a* axis and *c* face showing the packing layers. Dotted lines show the intra- and intermolecular interactions.

4. Experimental

4.1. General

Melting points are uncorrected. NMR spectra were recorded in $CDCl_3$ with tetramethylsilane as the internal standard for ^1H (250 MHz) unless otherwise stated. Mass spectra were recorded at an ionizing voltage of 70 eV. Chromatography was performed on flash silica gel (Merck) and TLC was carried out on 0.2-mm silica gel plates. All reagents and solvents were of commercial grade (Aldrich) and purified according to established convention.

4.1.1. 2-Hydroxy-4-octyloxyacetophenone (11).[29] A mixture of 2,4-dihydroxyacetophenone (5.00 g, 0.033 mol), octyliodide (5.6 ml, 0.033 mol) and K_2CO_3 (5.00 g) was refluxed in acetone (20 ml) for 3 h. To the reaction mixture was added water (20 ml) and extracted with ethyl acetate (3×30 ml). The organic layer was dried over $MgSO_4$, filtered and the solvent was evaporated under reduced pressure. The crude product was chromatographed using CH_2Cl_2 as eluting solvent to give the title compound **11** (R_f=0.13) as a light brown viscous liquid (6.88 g, 79%). ^{1}H NMR ($CDCl_3$, 250 MHz) δ 12.74 (s, 1H, OH), 7.6 (d, J=8.7 Hz, 1H), 6.5 (dd, J=8.7 Hz, J=2.4 Hz, 1H), 6.4 (s, 1H), 3.9 (t, J=6.6 Hz, 2H), 2.53 (s, 3H), 1.4 (m, 12H), 0.9 (t, J=5.59 Hz, 3H); $C_{16}H_{24}O_3$; EIMS (m/z) 264 (M^+).

4.1.2. *N*,*N*-Dibutylaminobenzene (3).[30] To the mixture of aniline **2** (0.008 mol, 0.72 ml), K_2CO_3 (2.18 g) and DMF (dry, 5 ml) heated at 120 °C was added butyliodide (3.05 g, 0.03 mol). It was heated at the same temperature for 10 h then the mixture was extracted with CH_2Cl_2, dried over $MgSO_4$, filtered and the solvent was evaporated under reduced pressure. The crude product was chromatographed using hexane/CH_2Cl_2 (4/1) as eluting solvent to give the title compound **3** as a light brown viscous liquid, (1.029 g, 82%). ^{1}H NMR ($CDCl_3$, 250 MHz) δ 7.17 (t, J=5.3 Hz, 2H), 6.6 (m, 3H), 3.25 (t, J=7.06 Hz, 4H), 1.6 (m, 4H), 1.3 (m, 4H), 0.9 (t, J=6.2 Hz, 6H); $C_{14}H_{23}N$; EIMS (m/z) 205 (M^+).

The following were similarly prepared.

4.1.3. *N*,*N*-Dioctylaminobenzene (4).[31] The crude product was chromatographed using hexane/CH_2Cl_2 (4/1) as eluting solvent to give the title compound **4** (R_f=0.48) as a brown viscous liquid (2.13 g, 84%). ^{1}H NMR ($CDCl_3$, 250 MHz) δ 7.18 (t, J=5.20 Hz, 2H), 6.67 (m, 3H), 3.20 (t, J=7.3 Hz, 4H), 1.7 (m, 4H), 1.35 (20H, m), 0.9 (t, J=6.1 Hz, 6H); $C_{22}H_{39}N$; EIMS (m/z) 317 (M^+).

4.1.4. *N*,*N*-Didodecylbenzamine (5). The crude product was chromatographed using hexane/CH_2Cl_2 (4/1) as eluting solvent to give the title compound **5** as a brown viscous liquid (2.77 g, 78%). ^{1}H NMR ($CDCl_3$, 250 MHz) δ 7.12 (t, J=5.25 Hz, 2H), 6.63 (m, 3H), 3.20 (t, J=7.25 Hz, 4H), 1.68 (m, 4H), 1.33 (m, 36H), 0.89 (t, J=6.19 Hz, 6H); $C_{30}H_{55}N$; EIMS (m/z) 430 (M^++1).

4.1.5. *N*,*N*-Dibutylamino benzaldehyde (6).[32] To an ice-cooled round-bottom flask containing $POCl_3$ (3.06 ml, 0.037 mol) was carefully added DMF (10 ml). The solution was warmed to room temperature and added **3** (3.3 g, 0.021 mol). The mixture was stirred for 4 h at 60 °C, then cooled to room temperature and ice was added to terminate the reaction. The mixture was extracted with CH_2Cl_2, dried over Na_2SO_4, filtered and the solvent was evaporated under reduced pressure. The crude product was chromatographed using hexane/CH_2Cl_2 (2/1) as eluting solvent to give the title compound **6** (R_f=0.34) as a brown viscous liquid (3.33 g, 68%). ^{1}H NMR ($CDCl_3$, 250 MHz) δ 9.67 (s, 1H), 7.7 (d, J=8.9 Hz, 2H), 6.6 (d, J=8.9 Hz, 2H), 3.35 (t, J=7.6 Hz, 4H), 1.56 (m, 4H), 1.37 (m, 4H), 0.95 (t, 7.24 Hz, 6H); $C_{15}H_{23}NO$; EIMS (m/z) 233 (M^+).

The following were similarly prepared.

4.1.6. *N*,*N*-Dioctylaminobenzaldehyde (7). The crude product was chromatographed using hexane/CH_2Cl_2 (2/1) as eluting solvent to give the title compound **7** (R_f=0.08) as a brown viscous liquid (4.5 g, 65%). ^{1}H NMR ($CDCl_3$, 250 MHz) δ 9.68 (s, 1H), 7.65 (d, J=8.5 Hz, 2H), 6.62 (d, J=8.5 Hz, 2H), 3.28 (t, J=7.2 Hz, 4H), 1.57 (m, 4H), 1.28 (m, 20H), 0.87 (t, J=6.30 Hz, 6H); $C_{23}H_{39}NO$; EIMS (m/z) 345 (M^+).

4.1.7. *N*,*N*-Didodecylaminobenzaldehyde (8). The crude product was chromatographed using hexane/CH_2Cl_2 (2/1) as eluting solvent to give the title compound **8** (R_f=0.11) as a brown viscous liquid (6.23 g, 67%). ^{1}H NMR ($CDCl_3$, 250 MHz) δ 9.75 (s, 1H), 7.60 (d, J=8.2 Hz, 2H), 6.59 (d, J=8.2 Hz, 2H), 3.30 (t, J=7.29 Hz, 4H), 1.50 (m, 4H), 1.21 (m, 36H), 0.84 (t, J=6.27 Hz, 6H); $C_{31}H_{55}NO$; EIMS (m/z) 458 (M^+).

4.1.8. 2-(4-Dibutylamino)phenyl-3-hydroxy-4*H*-chromen-4-one (21). To the solution of dibutylaminobenzaldehyde **6** (3.33 g, 0.0143 mol) and 2-hydroxyacetophenone **9** (1.95 g, 0.0143 mol) dissolved in DMF (dry, 5 ml) was added NaOMe (3.1 g, 0.057 mol) and the mixture was stirred at room temperature until a deep red colour was obtained (~5–8 h). Ethanol (20 ml) and NaOMe (0.7 g, 0.013 mol) were added, then the mixture was cooled to 0 °C, H_2O_2 (0.8 mol, 0.027 mol) was added carefully and heated at 120 °C for 10 min. The yellow mixture was then poured into water (50–100 ml) and neutralized with acetic acid. It was extracted with CH_2Cl_2, dried over Na_2SO_4, filtered and the solvent was evaporated under reduced pressure. The crude product was chromatographed using hexane/ethyl acetate (5/1) as eluting solvent to give the title compound **21** (R_f=0.53) as a yellow powder (0.97 g, 21%), mp 130–131.5 °C. [Found: C, 75.42, H, 7.12, N, 3.55. $C_{23}H_{27}NO_3$ C, 75.61, H, 7.39, N, 3.83%]; ^{1}H NMR ($CDCl_3$, 250 MHz) δ 8.21 (d, J=6.4 Hz, 1H), 8.15 (d, J=9.23 Hz, 2H), 7.63 (m, 1H), 7.53 (d, J=8.2 Hz, 1H), 7.38 (m, 1H), 6.72 (d, J=9.2 Hz, 2H), 3.34 (t, J=7.4 Hz, 4H), 1.60 (m, 4H), 1.35 (m, 4H), 0.96 (t, J=7.3 Hz, 6H); $C_{23}H_{27}NO_3$; EIMS (m/z) 366 (M^++1).

The following were similarly prepared.

4.1.9. 2-(4-Dioctylamino)phenyl-3-hydroxy-4*H*-chromen-4-one (22). The crude product was chromatographed using hexane/ethyl acetate (5/1) as eluting solvent to give the title compound **22** (R_f=0.65) as a light brown viscous liquid (1.2 g, 19%). [Found: C, 78.20, H, 8.79, N, 3.20. $C_{31}H_{43}NO_3$ C, 77.98, H, 9.01, N, 2.93%]; ^{1}H NMR (250 MHz, $CDCl_3$) δ 8.22 (d, J=7.9 Hz, 1H), 8.15 (d, J=9.2 Hz, 2H), 7.64 (m, 1H), 7.52 (d, J=7.6 Hz, 1H), 7.36 (m, 1H), 6.73 (d, J=9.2 Hz, 2H), 3.33 (t, J=7.4, 4H), 1.56 (m, 4H), 1.32 (m, 20H), 0.87 (t, J=6.6 Hz, 6H); $C_{31}H_{43}NO_3$; EIMS (m/z) 478 (M^++1).

4.1.10. 2-(4-Didodecylamino)phenyl-3-hydroxy-4*H*-chromen-4-one (23). The crude product was chromatographed using hexane/ethyl acetate (5/2) as eluting solvent to give the title compound **23** (R_f=0.75) as a light brown viscous liquid (1.6 g, 20%). [Found: C, 79.62, H, 9.85, N, 2.29. $C_{39}H_{59}NO_3$ C, 79.45, H, 10.01, N, 2.37%]; ^{1}H NMR

(250 MHz, $CDCl_3$) δ 8.1 (d, J=7.0 Hz, 1H), 8.12 (d, J=9.2 Hz, 2H), 7.59 (m, 1H), 7.5 (d, J=7.5 Hz, 1H), 7.32 (m, 1H), 6.68 (d, J=9.2 Hz, 2H), 3.35 (t, J=7.2 Hz, 4H), 1.58 (m, 4H), 1.30 (m, 36H), 0.83 (t, J=6.5 Hz, 6H); $C_{39}H_{59}NO_3$; EIMS (m/z) 590 (M^++1).

4.1.11. 2-(4-Dibutylamino)phenyl-3-hydroxy-7-methoxy-4*H*-chromen-4-one (24). The crude product was chromatographed using hexane/ethyl acetate (5/2) as eluting solvent to give the title compound **24** (R_f=0.5) as a yellow powder (0.76 g, 15%), mp 147–149 °C. [Found: C, 72.53, H, 7.52, N, 3.45. $C_{24}H_{29}NO_4$ C, 72.91, H, 7.34, N, 3.53%]; ^{1}H NMR (250 MHz, $CDCl_3$) δ 8.10 (d, J=9.1 Hz, 2H), 8.09 (d, J=8.8 Hz, 1H), 6.94 (m, 2H), 6.72 (d, J=9.1 Hz, 2H), 3.9 (s, 3H), 3.33 (t, J=7.3 Hz, 4H), 1.6 (m, 4H), 1.38 (m, 4H), 0.96 (t, J=7.3 Hz, 6H); $C_{24}H_{29}NO_4$; EIMS (m/z) 396 (M^++1).

4.1.12. 2-(4-Dioctylamino)phenyl-3-hydroxy-7-methoxy-4*H*-chromen-4-one (25). The crude product was chromatographed using hexane/ethyl acetate (5/2) as eluting solvent to give the title compound **25** (R_f=0.52) as a light brown viscous liquid (1.3 g, 19%). [Found: C, 75.43, H, 8.45, N, 2.82. $C_{32}H_{45}NO_4$ C, 75.73, H, 8.87, N, 2.76%]; ^{1}H NMR (250 MHz, $CDCl_3$) δ 8.12 (d, J=9.1 Hz, 2H), 8.09 (d, J=8.8 Hz, 1H), 6.93 (m, 2H), 6.9 (m, 2H), 6.42 (d, J=9.1 Hz, 2H), 3.91 (s, 3H), 3.32 (t, J=7.1 Hz, 4H), 1.61 (m, 4H), 1.28 (m, 20H), 0.88 (t, J=6.7 Hz, 6H); $C_{32}H_{45}NO_4$; EIMS (m/z) 508 (M^++1).

4.1.13. 2-(4-Didodecylamino)phenyl-3-hydroxy-7-methoxy-4*H*-chromen-4-one (26). The crude product was chromatographed using hexane/ethyl acetate (5/2) as eluting solvent to give the title compound **26** (R_f=0.47) as a light brown viscous liquid (1.51 g, 18%). [Found: C, 77.42, H, 9.53, N, 2.35. $C_{40}H_{61}NO_4$ C, 77.54, H, 9.85, N, 2.26%]; ^{1}H NMR (250 MHz, $CDCl_3$) δ 8.11 (d, J=9.1 Hz, 2H), 8.08 (d, J=8.8 Hz, 1H), 6.91 (m, 2H), 6.89 (m, 2H), 6.38 (d, J=9.1 Hz, 2H), 4.01 (s, 3H), 3.30 (t, J=7.1 Hz, 4H), 1.60 (m, 4H), 1.30 (m, 36H), 0.85 (t, J=6.6 Hz, 6H); $C_{40}H_{61}NO_4$; EIMS (m/z) 620 (M^++1).

4.1.14. 2-(4-Dibutylamino)phenyl-3-hydroxy-7-octyloxy-4*H*-chromen-4-one (27). The crude product was chromatographed using hexane/ethyl acetate (5/2) as eluting solvent to give the title compound **27** (R_f=0.8) as a light brown viscous liquid (1.1 g, 19%). [Found: C, 75.31, H, 8.54, N, 3.12. $C_{31}H_{43}NO_4$ C, 75.45, H, 8.72, N, 2.83%]; ^{1}H NMR (250 MHz, $CDCl_3$) δ 8.13 (d, J=9.1 Hz, 2H), 8.05 (d, J=8.7 Hz, 2H), 6.90 (m, 2H), 6.73 (d, J=9.1 Hz, 2H), 4.02 (t, J=6.2 Hz, 2H), 3.30 (t, J=7.3 Hz, 4H), 2.10 (m, 6H), 1.52 (m, 6H), 1.28 (m, 8H), 0.84 (m, 9H); $C_{31}H_{43}NO_4$; EIMS (m/z) 494 (M^++1).

4.1.15. 2-(4-Dioctylamino)phenyl-3-hydroxy-7-octyloxy-4*H*-chromen-4-one (28). The crude product was chromatographed using hexane/ethyl acetate (5/2) as eluting solvent to give the title compound **28** (R_f=0.9) as a brown viscous liquid (1.39 g, 17%). [Found: C, 77.53, H, 9.36, N, 2.44. $C_{39}H_{59}NO_4$ C, 77.35, H, 9.75, N, 2.31%]; ^{1}H NMR (250 MHz, $CDCl_3$) δ 8.1 (d, J=9.0 Hz, 2H), 8.08 (d, J=8.8 Hz, 2H), 6.92 (m, 2H), 6.70 (d, J=9.0 Hz, 2H), 4.04 (t, J=6.3 Hz, 2H), 3.35 (t, J=7.5 Hz, 4H), 2.13 (m, 6H), 1.55 (m, 6H), 1.31 (m, 30H), 0.88 (m, 9H); $C_{47}H_{75}NO_4$; EIMS (m/z) 606 (M^++1).

4.1.16. 2-(4-Didodecylamino)phenyl-3-hydroxy-7-octyloxy-4*H*-chromen-4-one (29). The crude product was chromatographed using hexane/ethyl acetate (5/2) as eluting solvent to give the title compound **29** (R_f=0.85) as a brown viscous liquid (1.47 g, 15%). [Found: C, 78.53, H, 10.71, N, 2.13. $C_{47}H_{75}NO_4$ C, 78.66, H, 10.46, N, 1.95%]; ^{1}H NMR (250 MHz, $CDCl_3$) δ 8.09 (d, J=9.1 Hz, 2H), 8.0 (d, J=8.8 Hz, 2H), 6.89 (m, 2H), 6.68 (d, J=9.1 Hz, 2H), 3.98 (t, J=6.3 Hz, 2H), 3.31 (t, J=7.5 Hz, 4H), 2.11 (m, 6H), 1.53 (m, 6H), 1.29 (m, 40H), 0.77 (m, 9H); $C_{47}H_{75}NO_4$; EIMS (m/z) 718 (M^++1).

4.2. X-ray analysis of 24

Single crystal measurements were performed on an Enraf–Nonius CAD4 four circle diffractometer equipped with graphite monochromator Cu Kα radiation. Semi-empirical (ψ scan) absorption corrections were applied. Structure was solved by direct methods (SHELXS97)[33] and refined by least-squares procedures on Fsqd (SHELXL97).[34] Non-hydrogen atom parameters were refined anisotropically. All hydrogen atoms were geometrically located and included using a riding model. The geometric calculations were carried out with the program Platon.[35] The crystal data and final parameters of the results of refinement are listed in Table 3. The molecular structure with numbering scheme and the packing arrangement of the molecules are presented in Figures 7 and 8. Selected bond lengths, bond angles and torsion angles are listed in Table 4. Fractional atomic coordinates, anisotropic displacement parameters and molecular dimensions have been deposited with the Cambridge Crystallographic data centre (CCDC 651344).

Table 3. Crystal data and structure refinement parameters for **24**

Crystal data	
Formula	$C_{24}H_{29}NO_4$
Crystal habit	Brown, prism
Crystal size (mm)	0.30×0.33×0.48
Symmetry	Monoclinic, $P2_1/n$
Unit cell dimensions (Å,°)	a=15.7075(17)
	b=15.3951(14)
	c=18.458(2)
	β=105.633(9)
V (Å^3), Z	4298.4(8), 8
D_{calcd} (g cm^{-3}), M	1.222, 395.48
λ (Cu Kα) (Å), Scan type	1.54184, ω–2θ
μ (Cu Kα) (mm^{-1})	0.664
T_{min}, T_{max} (%)	78.2, 81.9
Experimental data	
$2\theta_{max}$ (°)	141.58
Index ranges	$-18\le h\le 19$; $0\le k\le 18$; $-22\le l\le 0$
Reflections collected	7330
Reflections independent/used in refinement	7330/7112
No. of refined parameters	524
R/R_w values	0.0803/0.2234
GOF on F^2	1.02
Final shift	0.00
$(\Delta\rho)_{min}$, $(\Delta\rho)_{max}$ (e Å^{-3})	−0.553, 0.761

Table 4. Selected geometrical parameters (°, Å) of **24**

	Molecule A	Molecule B
C11–O4	1.423(4)	1.423(4)
C7–O4	1.352(4)	1.359(4)
C4–C10	1.440(5)	1.444(5)
C4–O3	1.241(4)	1.242(4)
C3–O2	1.360(4)	1.358(4)
C2–C12	1.468(4)	1.454(5)
C15–N1	1.384(4)	1.373(4)
C18–N1	1.445(5)	1.457(4)
C22–N1	1.468(5)	1.456(4)
C3–C2–C12	128.4(3)	128.2(3)
C2–C3–O2	120.2(3)	119.6(3)
O3–C4–C10	123.5(4)	123.2(4)
O4–C7–C8	124.9(4)	124.3(4)
N1–C15–C16	122.4(3)	123.2(3)
C18–N1–C22	115.1(3)	116.8(3)
C7–O4–C11	118.9(3)	118.7(3)
C8–C7–O4–C11	−3.7(6)	−12.5(6)
O1–C2–C12–C17	−7.4(5)	−24.2(5)
C14–C15–N1–C18	−3.2(6)	−12.4(5)
C19–C18–N1–C22	−89.2(4)	−93.0(4)
C23–C22–N1–C18	−87.2(5)	−82.9(4)

Acknowledgements

We thank TUBITAK for supporting this work (TBAG 2378-103T122).

References and notes

1. (a) Sengupta, P. K.; Kasha, M. *Chem. Phys. Lett.* **1979**, *68*, 382–385; (b) Woolfe, G. E.; Thistlewaithe, P. G. *J. Am. Chem. Soc.* **1981**, *103*, 6916–6923; (c) Chou, P.; McMorrow, D.; Aartsma, T. J.; Kasha, M. *J. Phys. Chem.* **1984**, *88*, 4596–4599; (d) McMorrow, D.; Kasha, M. *J. Am. Chem. Soc.* **1983**, *105*, 5133–5134; (e) McMorrow, D.; Kasha, M. *J. Phys. Chem.* **1984**, *88*, 2235–2243; (f) Strandjord, A. J. G.; Barbara, P. F. *J. Phys. Chem.* **1985**, *89*, 2355–2361.
2. Sytnik, A.; Gormin, D.; Kasha, M. *Proc. Natl. Acad. Sci. U.S.A.* **1994**, *91*, 11968–11972.
3. Sarkar, M.; Ray, J. G.; Sengupta, P. K. *Spectrochim. Acta Part, A* **1996**, *52*, 275–278.
4. Dharia, J. R.; Johnson, K. F.; Schlenoff, J. B. *Macromolecules* **1994**, *27*, 5167–5172.
5. Formosinho, J. S.; Arnaut, G. L. *J. Photochem. Photobiol., A: Chem.* **1993**, *75*, 21–48.
6. (a) Chou, P.-T.; Martinez, M. L.; Clements, J. H. *J. Phys. Chem.* **1993**, *97*, 2618–2622; (b) Swiney, T. C.; Kelley, F. D. *J. Chem. Phys.* **1993**, *99*, 211–221; (c) Ormson, S. M.; Brown, R. G.; Vollmer, F.; Rettig, W. *J. Photochem. Photobiol., A: Chem.* **1994**, *81*, 65–72; (d) Klymchenko, A. S.; Ozturk, T.; Pivovarenko, V. G.; Demchenko, A. P. *Can. J. Chem.* **2001**, *79*, 358–363; (e) Klymchenko, A. S.; Ozturk, T.; Pivovarenko, V. G.; Demchenko, A. P. *Tetrahedron Lett.* **2001**, *42*, 7967–7970; (f) Klymchenko, A. S.; Ozturk, T.; Demchenko, A. P. *Tetrahedron Lett.* **2002**, *43*, 7079–7082; (g) Klymchenko, A. S.; Pivovarenko, V. G.; Ozturk, T.; Demchenko, A. P. *New J. Chem.* **2003**, *27*, 1336–1343; (h) Klymchenko, A. S.; Demchenko, A. P. *Phys. Chem. Chem. Phys.* **2003**, *5*, 461–468.
7. Roshal, A. D.; Grigorovich, A. V.; Doroshenko, A. O.; Pivovarenko, V. G.; Demchenko, A. P. *J. Phys. Chem. A* **1998**, *102*, 5907–5914.
8. (a) Pivovarenko, V. G.; Tuganova, A. V.; Klymchenko, A. S.; Demchenko, A. P. *Cell. Mol. Biol. Lett.* **1997**, *2*, 355–364; (b) Klymchenko, A. S.; Demchenko, A. P. *Langmuir* **2002**, *18*, 5637–5639.
9. (a) Bondar, O. P.; Pivovarenko, V. G.; Rowe, E. S. *Biochem. Biophys. Acta* **1998**, *1369*, 119–130; (b) Duportail, G.; Klymchenko, A. S.; Mely, Y.; Demchenko, A. P. *FEBS Lett.* **2001**, *508*, 196–200; (c) Duportail, G.; Klymchenko, A. S.; Mely, Y.; Demchenko, A. P. *J. Fluorescence* **2002**, *12*, 181–185.
10. (a) Chattopadhyay, A.; London, E. *Biochemistry* **1987**, *26*, 39–45; (b) Abrams, F. S.; London, E. *Biochemistry* **1993**, *32*, 10826–10831.
11. Klymchenko, A. S.; Duportail, G.; Ozturk, T.; Pivovarenko, V. G. *Chem. Biol.* **2002**, *9*, 1199–1206.
12. Banerjee, A.; Sengupta, P. K. *Chem. Phys. Lett.* **2006**, *424*, 379–386.
13. Barroso, M.; Chattopadhyay, N.; Klymchenko, A. S.; Demchenko, A. P.; Arnaut, L. G.; Formosinho, S. J. *J. Phys. Chem. A* **2006**, *110*, 13419–13424.
14. Algar, J.; Flynn, J. *Proc. R. Irish Acad.* **1934**, *B42*, 1–5.
15. Shynkar, V. V.; Klymchenko, A. S.; Piemont, E.; Demchenko, A. P.; Mely, Y. *J. Phys. Chem. A* **2004**, *108*, 8151–8159.
16. Lakowics, J. R. *Principles of Fluorescence Spectroscopy*; Kluwer: New York, NY, 1999.
17. Klymchenko, A. S.; Duportail, G.; Demchenko, A. P.; Mely, Y. *Biophys. J.* **2004**, *86*, 2929–2941.
18. Klymchenko, A. S.; Mely, Y.; Demchenko, A. P.; Duportail, G. *Biochim. Biophys. Acta* **2004**, *1665*, 6–19.
19. Cang, H.; Brace, D. D.; Fayer, M. D. *J. Phys. Chem. B* **2001**, *105*, 10007–10015.
20. Dutt, G. B. *J. Phys. Chem. B* **2003**, *107*, 10546–10551.
21. Maciejewski, A.; Kubicki, J.; Dobek, K. *J. Phys. Chem. B* **2003**, *107*, 13986–13999.
22. Matzinger, S.; Hussey, D. M.; Fayer, M. D. *J. Phys. Chem. B* **1998**, *102*, 7216–7224.
23. Jiang, R. W.; Ye, W. C.; Woo, K. Y.; Du, J.; Che, C. T.; But, P. P. H.; Mak, T. C. W. *J. Mol. Struct.* **2002**, *642*, 77–84.
24. Jiang, R. W.; He, Z. D.; But, P. P. H.; Chan, Y. M.; Ma, S. C.; Mak, T. C. W. *Chem. Pharm. Bull.* **2001**, *49*, 1166–1169.
25. Kendi, E.; Özbey, S.; Bozdağ, O.; Ertan, R. *Acta Crystallogr.* **2000**, *C56*, 457–458.
26. Özbey, S.; Kendi, E.; Ayhan-Kilcigil, G.; Ertan, R. *Acta Crystallogr.* **1999**, *C55*, 678–680.
27. Etter, M. C.; Lipkowska, Z. U.; Baer, S.; Barbara, P. F. *J. Mol. Struct.* **1986**, *144*, 155–167.
28. Shoja, M. *Acta Crystallogr.* **1989**, *C45*, 828–829.
29. Horie, T.; Tsukayama, M.; Kourai, H.; Yokoyama, C.; Furukawa, M.; Yoshimoto, T.; Yamamoto, S.; Watanabekohno, S.; Ohata, K. *J. Med. Chem.* **1986**, *29*, 2256–2262.
30. Srivastava, S. K.; Chauhan, P. M. S.; Bhaduri, A. P. *Synth. Commun.* **1999**, *29*, 2085–2091.
31. Fujita, K.-I.; Li, Z.; Ozekib, N.; Yamaguchib, R. *Tetrahedron Lett.* **2003**, *44*, 2687–2690.
32. Plater, M. J.; Jackson, T. *Tetrahedron* **2003**, *59*, 4673–4685.
33. Sheldrick, G. M. *SHELXS97. Program for Crystal Structure Solution*; University of Göttingen: Göttingen, Germany, 1997.
34. Sheldrick, G. M. *SHELXL97. Program for Crystal Structure Refinement*; University of Göttingen: Göttingen, Germany, 1997.
35. Spek, A. L. *Acta Crystallogr.* **1990**, *A46*, C34–C36.